



# Effect of Microcracks in the Annular Groove Region of a Tungsten Alloy Kinetic Energy Penetrator

by Todd W. Bjerke and Brett R. Sorensen

ARL-RP-85

September 2004

A reprint from the *Proceedings of the International Ballistics Symposium*, Adelaide, South Australia, 12–23 April 2004.

[www.chinatungsten.com](http://www.chinatungsten.com)

## **NOTICES**

### **Disclaimers**

The findings in this report are not to be construed as an official Department of the Army position unless so designated by other authorized documents.

Citation of manufacturer's or trade names does not constitute an official endorsement or approval of the use thereof.

Destroy this report when it is no longer needed. Do not return it to the originator.

# Army Research Laboratory

Aberdeen Proving Ground, MD 21005-5066

---

---

ARL-RP-85

September 2004

---

---

## Effect of Microcracks in the Annular Groove Region of a Tungsten Alloy Kinetic Energy Penetrator

Todd W. Bjerke and Brett R. Sorensen  
Weapons and Materials Research Directorate, ARL

A reprint from the *Proceedings of the International Ballistics Symposium*, Adelaide, South Australia, 12–23 April 2004.

## Report Documentation Page

*Form Approved*  
OMB No. 0704-0188

Public reporting burden for this collection of information is estimated to average 1 hour per response, including the time for reviewing instructions, searching existing data sources, gathering and maintaining the data needed, and completing and reviewing the collection information. Send comments regarding this burden estimate or any other aspect of this collection of information, including suggestions for reducing the burden, to Department of Defense, Washington Headquarters Services, Directorate for Information Operations and Reports (0704-0188), 1215 Jefferson Davis Highway, Suite 1204, Arlington, VA 22202-4302. Respondents should be aware that notwithstanding any other provision of law, no person shall be subject to any penalty for failing to comply with a collection of information if it does not display a currently valid OMB control number.  
**PLEASE DO NOT RETURN YOUR FORM TO THE ABOVE ADDRESS.**

<b>1. REPORT DATE (DD-MM-YYYY)</b> September 2004		<b>2. REPORT TYPE</b> Reprint		<b>3. DATES COVERED (From - To)</b> October 2003–March 2004	
<b>4. TITLE AND SUBTITLE</b> Effect of Microcracks in the Annular Groove Region of a Tungsten Alloy Kinetic Energy Penetrator				<b>5a. CONTRACT NUMBER</b>	
				<b>5b. GRANT NUMBER</b>	
				<b>5c. PROGRAM ELEMENT NUMBER</b>	
<b>6. AUTHOR(S)</b> Todd W. Bjerke and Brett R. Sorensen				<b>5d. PROJECT NUMBER</b> 611102.AH42	
				<b>5e. TASK NUMBER</b>	
				<b>5f. WORK UNIT NUMBER</b>	
<b>7. PERFORMING ORGANIZATION NAME(S) AND ADDRESS(ES)</b> U.S. Army Research Laboratory ATTN: AMSRD-ARL-WM-T Aberdeen Proving Ground, MD 21005-5066				<b>8. PERFORMING ORGANIZATION REPORT NUMBER</b> ARL-RP-85	
<b>9. SPONSORING/MONITORING AGENCY NAME(S) AND ADDRESS(ES)</b>				<b>10. SPONSOR/MONITOR'S ACRONYM(S)</b>	
				<b>11. SPONSOR/MONITOR'S REPORT NUMBER(S)</b>	
<b>12. DISTRIBUTION/AVAILABILITY STATEMENT</b> Approved for public release; distribution is unlimited.					
<b>13. SUPPLEMENTARY NOTES</b> A reprint from the <i>Proceedings of the International Ballistics Symposium</i> , Adelaide, South Australia, 12–23 April 2004.					
<b>14. ABSTRACT</b> The influence of microcracks in the annular groove region of a kinetic energy penetrator is examined through a combined theoretical, experimental, and computational study. Microcracks resulting from plastic deformation are quantified for a typical penetrator made from tungsten alloy (WA). The effect of existing and proposed annular groove geometries on the stress field near the penetrator surface is determined using finite element techniques, and the effect of the various stress fields on the critical flaw size is examined. Recommendations of microcrack size and groove geometry are made to improve the fracture resistance of conventional WA long rod penetrators.					
<b>15. SUBJECT TERMS</b> kinetic energy penetrators, fracture					
<b>16. SECURITY CLASSIFICATION OF:</b>			<b>17. LIMITATION OF ABSTRACT</b>	<b>18. NUMBER OF PAGES</b>	<b>19a. NAME OF RESPONSIBLE PERSON</b> Brett Sorensen
<b>a. REPORT</b> UNCLASSIFIED	<b>b. ABSTRACT</b> UNCLASSIFIED	<b>c. THIS PAGE</b> UNCLASSIFIED			UL

# EFFECT OF MICROCRACKS IN THE ANNULAR GROOVE REGION OF A TUNGSTEN ALLOY KINETIC ENERGY PENETRATOR

**Todd W. Bjerke and Brett R. Sorensen**

U.S. Army Research Laboratory  
Weapons and Materials Research Directorate  
Terminal Effects Division  
Aberdeen Proving Ground, MD 21005

The influence of microcracks in the annular groove region of a kinetic energy penetrator is examined through a combined theoretical, experimental, and computational study. Microcracks resulting from plastic deformation are quantified for a typical penetrator made from tungsten alloy (WA). The effect of existing and proposed annular groove geometries on the stress field near the penetrator surface is determined using finite element techniques, and the effect of the various stress fields on the critical flaw size is examined. Recommendations of microcrack size and groove geometry are made to improve the fracture resistance of conventional WA long rod penetrators.

## **Introduction**

Fracture of kinetic energy (KE) penetrators has been observed in both medium- and large-caliber penetrators. A common feature between these penetrators is the annular grooves used to transfer shear from the sabot to the penetrator during launch. This relatively sharp feature acts as a stress concentration and can lead to Mode I fracture in the penetrator under certain loading conditions from either the cannon launch or the terminal ballistic engagement with the armored vehicle. Understanding and predicting this mode of failure in high-density metals is critical to the proper design of effective long rod penetrators. This paper examines the state of stress and strain at the root of several groove configurations for a KE penetrator made from a tungsten-sintered alloy. The existence of microcracks near the surface of the material, resulting from an applied load, is first examined through experiments. The conditions necessary for the microcracks to cause macroscopic fracture in this class of material is then considered. Finally, the results from a series of numerical simulations that model several groove configurations are presented to identify the significance of microcracking on overall penetrator structural integrity.

## Beam Impact Experiments

A key parameter for the modeling presented in this paper is the degree of microcracking, if any, that exists in the groove region of the penetrator material. To address this issue, a series of experiments were performed to determine if microcracks do in fact exist prior to the formation of a large, unstable crack, and how far beneath the material surface the microcracks extend. The experimental configuration used was a dynamic beam impact test, depicted in Fig 1. The beam-shaped WA test specimen was struck with a WA projectile of similar composition to induce a dynamic Mode I fracture event, initiating on the side opposite that struck by the projectile. During dynamic beam flexure but prior to failure (i.e., unstable macroscopic crack growth), small microcracks that either pre-exist or form during dynamic loading will open and possibly remain open for posttest inspection. It is through posttest optical inspection of the region near the fracture surface that the existence of microcracks can be verified, and their depth determined.

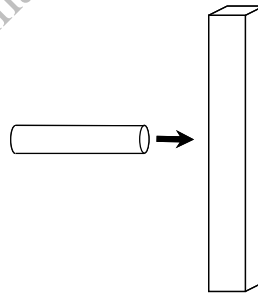


FIGURE 1. Schematic depiction of the beam impact experiments.

The experiments were performed using a 93% (by weight) tungsten, 5.6% nickel, and 1.4% iron WHA. The bulk density was  $17.76 \text{ g/cm}^3$ . The original material was in the form of a bar that had been swaged to 20% reduction in area and aged. The quasi-static ultimate tensile true stress was 1.425 GPa, with a logarithmic strain of 12.5%, and the quasi-static yield stress was 1.19 GPa (these were furnished by the material supplier). The dilatational and shear wave speeds were measured to be 5163 and 2824 m/s using an ultrasound technique. The material elastic modulus and Poisson's ratio were 365 GPa and 0.29, respectively. These were determined from the measured wave speeds. Beam specimens were cut from a large WHA bar using conventional machining techniques similar to those used to cut grooves in KE penetrators. The beam specimen had a length of 127 mm and a square cross section with height and width of 9 mm each. The length and diameter of the projectile were 44.5 and 8.9 mm, respectively. The impact speed was 55 m/s.

The rear surface region of the impacted beam specimens near the fracture plane was examined with a scanning electron microscope to confirm the presence of micro-

cracks and to estimate microcracking depth. A typical image of this region is shown in Fig 2a. The fracture plane is located just beyond the bottom of the image. Significant microcracking is evident, with the microcracks oriented perpendicular to the beam longitudinal axis. The maximum crack opening was determined to be approximately 1.7  $\mu\text{m}$ . Images of the beam surface taken far from the region of fracture (not shown) did not show any evidence of microcracking, suggesting that the large tensile stress near the fracture plane of the beam was responsible for either opening existing microcracks or causing them to form.

The depth of the microcracking was estimated from additional micrographs taken along the region where the macroscopic fracture event initiated. Fig 2b shows a typical surface topography of this region. The beam specimen was rotated into the plane of the image by  $40^\circ$  to obtain the necessary perspective to estimate microcracking depth. The circled area of Fig 2b shows the remnants of a microcrack. As can be seen, the crevasse has a depth of one tungsten grain, or  $\sim 40 \mu\text{m}$ . The formation of microcracks in a tungsten-sintered alloy during tensile loading was discussed in detail by Weerasooriya [1], who found the grain-to-grain contact to be the weakest portion of the alloy, and therefore the first to fail. An identical mechanism is likely responsible for the microcracking observed in the recovered beam impact specimens.

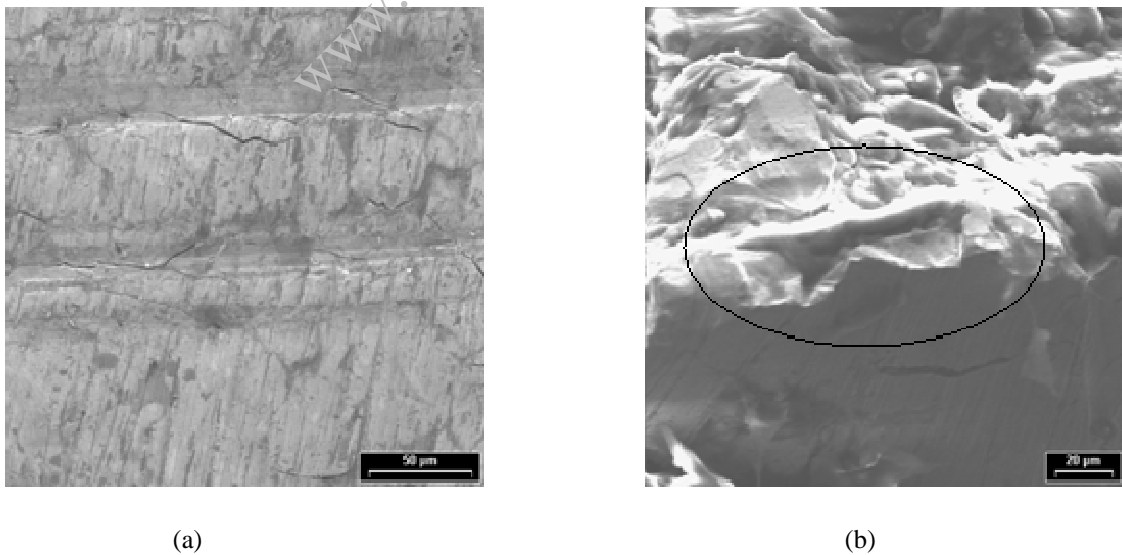


FIGURE 2. Scanning electron microscope image of the beam specimen. (a) Surface near the fracture plane. Actual fracture plane is located just beyond the bottom of the image. (b) Oblique view of a microcrack interacting with the main fracture plane. Circled region identifies the microcrack of interest.

The beam impact experiments verify that microcracks can exist in tungsten-sintered alloys when subjected to tensile loads below the catastrophic limit. Furthermore, microcracking appears to penetrate to a depth of one grain diameter below the

machined surface. This provides the estimates of microcrack length needed for the elastic-plastic fracture mechanics and finite element analyses which are presented next.

### Elastic-Plastic Fracture Mechanics Considerations

The observations from the beam impact experiments confirmed the presence of microcracks, having a depth of approximately one tungsten grain diameter ( $40 \mu\text{m}$ ) below the surface. In the context of a KE penetrator, these microcracks will exist in the groove region of the penetrator, which is subject to macroscopic elastic-plastic deformation. Hutchinson [2] and Rice and Rosengren [3] each developed crack tip solutions for materials capable of plastic behavior. Introducing plasticity eliminated the possibility for using linear elastic fracture mechanics (LEFM) in the direct vicinity of the crack tip. Far from the crack tip (but still in the crack tip region) LEFM does apply. However, the region near the crack tip is characterized by the plastic solutions of Hutchinson, Rice, and Rosengren, and is referred to as the HRR field. The stress field ahead of a sharp crack in an elastic-plastic material is shown in Fig 3. The decrease in stress very close to the crack tip, denoted as RJ, is due to crack tip blunting [4].

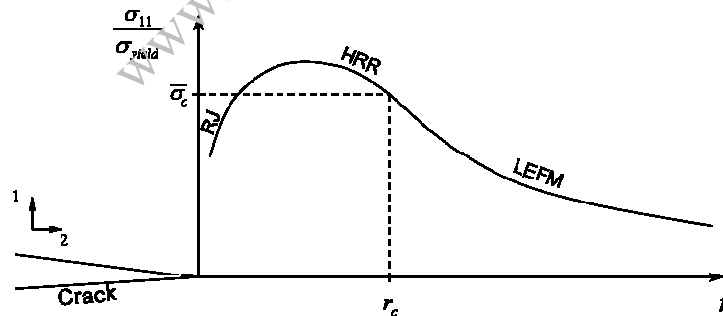


FIGURE 3. Schematic depiction of the opening stress field ahead of a sharp crack.

Application of LEFM and the HRR field to determine the fracture initiation criterion for low temperature mild steel was performed by Ritchie, Knott, and Rice [5]. At low temperatures, mild steel (BCC crystal structure) fractures by brittle grain cleavage [6]. This crystal structure and mode of failure are similar to those of the tungsten-sintered alloy examined in this study. Ritchie, Knott and Rice found that a critical stress must be exceeded at a certain distance ahead of the crack tip for fracture initiation to occur. The critical stress and distance are denoted in Fig 3 as  $r_c$  and  $\bar{\sigma}_c$ , respect-

tively. For brittle fracture of mild steel,  $r_c$  was found to be two grain diameters. It was hypothesized by Ritchie, Knott, and Rice that the driving force necessary for grain cleavage ( $\bar{\sigma}_c$ ) must extend beyond the first grain due to the random grain orientation of the material and the preferential cleavage directions of BCC grains. Should the first grain cleave, the crack tip would likely be in front of a grain, oriented in a way that would be less favorable to cleavage. Hence, an *overabundance* of driving energy is needed for macroscopic fracture to occur. A similar argument for unstable crack initiation is proposed for the tungsten-sintered alloy examined here. In what follows, a finite element technique is used to examine both the crack tip driving energy for an elastic-plastic material (the J-integral) as well as the extent to which the stress field penetrates below the material surface for various groove configurations and microcrack depths. The intent here is not to quantify the fracture criterion, but rather to examine the relative effects of various groove configurations and microcrack depths.

### Finite Element Analyses

The state of stress and strain in the groove region of a KE penetrator was examined using the finite element code ANSYS. For large-caliber penetrators, the grooves typically have a  $7^\circ$  driving land and a  $45^\circ$  clearance flank with blend radii to the minor diameter, as shown in Fig 4. Because these radii act as stress risers under bending loads, changing to a triradial blend between the  $7$  and  $45^\circ$  surfaces has been demonstrated to decrease bending stresses by 20-25%; thus, possibly decreasing the energy required to initiate an existing flaw into a propagating crack. An initial, baseline numerical simulation was performed using grooves with a single and triradial blend on a penetrator subjected to quasi-static three-point bend loading. To simplify the finite element model, a harmonic, axisymmetric element was used. While this reduced problem size and permitted adequate mesh resolution, the harmonic element limited the analysis to linear elastic response. This initial analysis indicated that the triradial profile reduced maximum bending stresses by 17%, but the stress profiles were the same for locations  $100\ \mu\text{m}$  or greater below the surface. Furthermore, the stresses were several times the yield stress, indicating the need to introduce material plasticity into the simulations.

Subsequent simulations utilized modeling techniques that permitted material plasticity and the inclusion of sharp cracks. A plane stress approach was used and the geometry was mirrored about the axis of symmetry. By setting element thickness to maintain cross-sectional inertia of the “circular” penetrator, deflections resulting from bending loads would be accurate in the “rectangular” penetrator model. Finally, because the distance to the neutral axis was also preserved, stresses would also be maintained. A detailed analysis of this modeling technique is presented in Sorensen [7].

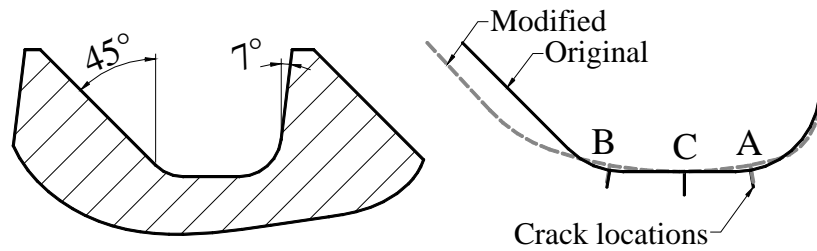
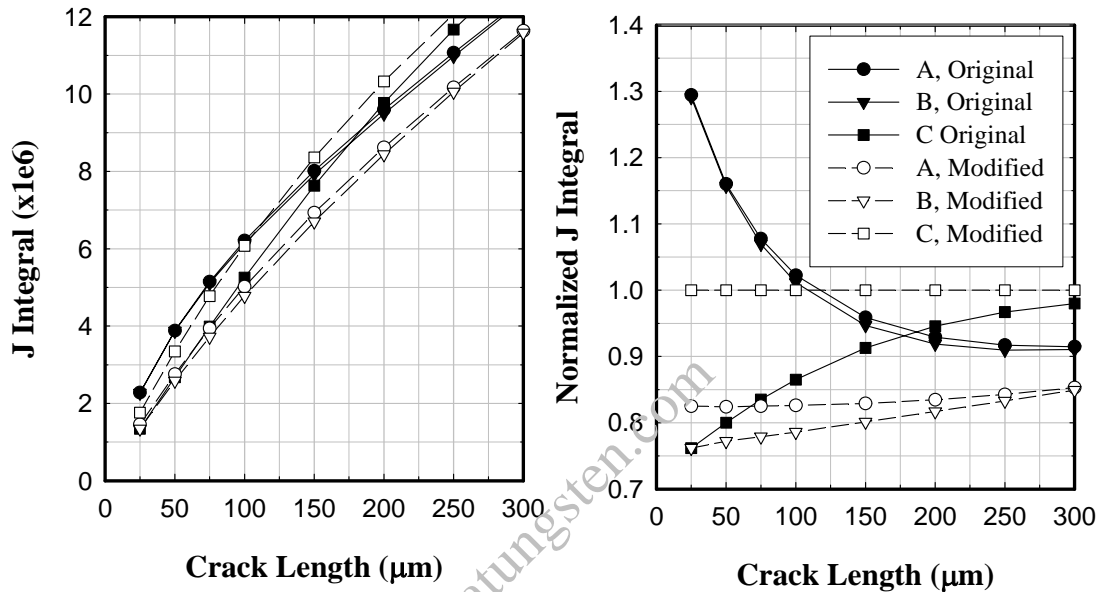


FIGURE 4. Groove profile illustrating the 7 and 45° flanks and a superposition of the original and modified groove profiles illustrating crack locations.

Before jumping straight into the complexity of elastic-plastic numerical simulations with pre-existing cracks, a set of linear elastic simulations with cracks of a given size were first performed. This provided an understanding of the structural response to specific flaws, or more specifically, to flaw location and size. For the elastic analysis, infinitely sharp cracks were introduced into three locations of each groove profile, as shown in Fig 4. These locations were selected because they coincide with the maximum stress locations in both groove profiles: A and B for the original groove and C for the modified groove. In each case, the crack was normal to the surface and at the same axial locations for either groove profile.

Results from these simulations are shown in Fig 5. In Fig 5a, the J-integral is plotted as a function of crack length and illustrates global response to crack length. In Fig 5b, the J-integrals are normalized by the J-integral from crack C for the modified profile and show relative response to crack length and location. Note that J is proportional to  $K_I^2$ , where  $K_I$  is the Mode I stress intensity factor because the analysis is limited to linear elastic material behavior [8]. The primary observation is that, as expected, the J-integral increases with crack length. Secondly, depending on location and extent of stress risers, the relative magnitude of maximum stress intensity varies by up to 30% between the two grooves. However, if critical flaw size is in excess of 40  $\mu\text{m}$  (i.e., one tungsten grain diameter), this difference decreases to 15%. Therefore, from a LEFM analysis, the difference between the two profiles may be irrelevant, particularly if there is an *overabundance* of driving energy.

To begin to understand the effects of plasticity, two limited numerical analyses were performed using a bilinear elastic-plastic model. The first analysis examined the plastic response of the penetrator without the imposed flaw. The results showed that for the applied loading, maximum tensile plastic strains of 4.5% and 3.0% were present for the original and modified grooves, respectively. However, while the plastic strains in the original groove were 50% higher, the extent of the plastic strain field in excess of 3.0% (i.e., the size of the plastic zone) was smaller for the modified groove.



(b)

FIGURE 5. Results from linear-elastic fracture analysis.

The second numerical analysis examined the effects of crack size with plasticity present. Here, only the crack location in the maximum stress riser was examined for crack sizes up to 100 μm (locations A and C for the original and modified grooves, respectively). Furthermore, the applied load had to be reduced 50% to avoid instabilities during solution. Table 1 presents results in terms of the maximum effective plastic strain at the crack tip and the extent of the plastic strain field beyond the crack tip as a function of crack length. The results in Table 1 indicate that there is a demarcation for plastic strain and plastic zone extent with respect to crack length between 30 to 50 μm. For crack lengths greater than 50 μm, plastic strain and its extent are moving toward an asymptote, and the differences between the two grooves are decreasing. Furthermore, the extent of the plastic zone is in excess of the average grain size. The results do show, however, that for small cracks, the maximum strain and plastic zone size are slightly smaller for the modified groove design. Hence, if the fracture initiation criterion of Ritchie, Knott, and Rice discussed earlier is true for tungsten-sintered materials, use of the modified groove geometry may result in a penetrator design more resistant to fracture. However the differences for the larger crack sizes may be sufficiently small to have negligible influence on fracture initiation.

TABLE 1. Plastic Strain Field Parameters for Various Crack Sizes

Crack Length ( $\mu\text{m}$ )	Max. Effective Plastic Strain (%)		Plastic Strain Field Size ( $\mu\text{m}$ )	
	Original Groove	Modified Groove	Original Groove	Modified Groove
25	69	60	35	25
50	92	87	75	55
75	105	106	100	90
100	114	121	110	115

## Conclusions

The existence of microcracks in the high-stress region surrounding a macroscopic fracture in a 93% tungsten-sintered alloy was verified through an experimental technique. Their presence suggests that a fracture initiation criterion that includes not only maximum stress or strain near the crack tip, but also the size of the region encompassed by high stresses or strains may apply. Elastic-plastic numerical simulations of various groove configurations with pre-existing microcracks indicated a modified groove geometry would slightly decrease the maximum strain and size of the plastic zone; however, the decrease may not be sufficient to affect fracture initiation.

## References

1. Weerasooriya, T., "Deformation and failure behavior of a tungsten heavy alloy under tensile loading at different strain rates", Proceedings of the Society for Experimental Mechanics Annual Conference and Exhibition, Charlotte, North Carolina June 2-4, 2003.
2. Hutchinson, J.W., "Singular behavior at the end of a tensile crack in a hardening material", *Journal of the Mechanics and Physics of Solids*, 16, 13-31, 1968.
3. Rice, J.R., and Rosengren, G.F., "Plane strain deformation near a crack tip in a power-law hardening material", *Journal of the Mechanics and Physics of Solids*, 16, 1-12, 1968.
4. Rice, J.R., and Johnson, M.A., *Inelastic Behavior of Solids* (edited by Kanninen, M.F., Adler, W., Rosenfield, A., and Jaffe, R.), p. 641. McGraw-Hill Publishers, New York, 1970.
5. Knott, J.F., "Some effects of hydrostatic tension on fracture behavior of mild steel.", *Journal of the Iron and Steel Institute*, 204, 104- & part 2, 1966.
6. Ritchie, R.O., Knott, J.F., and Rice, J.R., "On the relationship between critical tensile stress and fracture toughness in mild steel", *Journal of the Mechanics and Physics of Solids*, 21, 395-410, 1973.
7. Sorensen, B.R., "Analysis of a Proposed Redesign of the Kinetic Energy Penetrator Groove Profile to Reduce Bending Stresses", Proceedings of the 2002 ANSYS User's Conference, Pittsburgh, PA, May 2002.
8. Anderson, T.L., *Fracture Mechanics: Fundamentals and Applications*, CRC Press, Inc., 1995, New York, New York.

NO. OF  
COPIES ORGANIZATION

- 1 DEFENSE TECHNICAL  
(PDF INFORMATION CTR  
ONLY) DTIC OCA  
8725 JOHN J KINGMAN RD  
STE 0944  
FT BELVOIR VA 22060-6218
- 1 US ARMY RSRCH DEV &  
ENGRG CMD  
SYSTEMS OF SYSTEMS  
INTEGRATION  
AMSRD SS T  
6000 6TH ST STE 100  
FORT BELVOIR VA 22060-5608
- 1 INST FOR ADVNCD TCHNLGY  
THE UNIV OF TEXAS  
AT AUSTIN  
3925 W BRAKER LN STE 400  
AUSTIN TX 78759-5316
- 1 US MILITARY ACADEMY  
MATH SCI CTR EXCELLENCE  
MADN MATH  
THAYER HALL  
WEST POINT NY 10996-1786
- 1 DIRECTOR  
US ARMY RESEARCH LAB  
IMNE AD IM DR  
2800 POWDER MILL RD  
ADELPHI MD 20783-1197
- 3 DIRECTOR  
US ARMY RESEARCH LAB  
AMSRD ARL CI OK TL  
2800 POWDER MILL RD  
ADELPHI MD 20783-1197
- 3 DIRECTOR  
US ARMY RESEARCH LAB  
AMSRD ARL CS IS T  
2800 POWDER MILL RD  
ADELPHI MD 20783-1197

NO. OF  
COPIES ORGANIZATION

ABERDEEN PROVING GROUND

- 1 DIR USARL  
AMSRD ARL CI OK TP (BLDG  
4600)

NO. OF  
COPIES ORGANIZATION

ABERDEEN PROVING GROUND

20 DIR USARL  
AMSRD ARL WM TD  
T BJERKE (10 CPS)  
AMSRD ARL TC  
B SORENSEN (10 CPS)

[www.chinatungsten.com](http://www.chinatungsten.com)